Curr Radiol Rep (2016) 4:6
DOI 10.1007/s40134-015-0134-8

"Weak Links" of the Pediatric Skeleton: Common Foci for Disease and Trauma. Part 1: The Link Between Bone and Cartilage

Sagar Wagle[1] · Andrew S. Phelps[1] · John D. MacKenzie[1]

Published online: 5 January 2016

Abstract In this article, we review recent updates in the radiologic imaging of injuries to the pediatric skeleton. In part 1, we focus on the link between cartilage and bone. Part 2 focuses on other areas of the developing skeleton that are susceptible to injury. Over the past 5 years, new and interesting research has helped us to better understand pediatric skeletal disease processes and how to image these "weak links." These cartilage–bone interfaces are unique to the pediatric skeleton, and understanding of this anatomy is critical in the performance and interpretation of pediatric musculoskeletal imaging examinations.

Keywords Pediatrics · Skeleton · Imaging

Introduction

The "weakest links" in the pediatric skeleton are primarily found at transitions in tissue types (Table 1). Both acute and chronic (e.g., repetitive motion) injuries to the pediatric skeleton tend to occur at the boundaries between bone, cartilage, and fibrous tissue. However, these areas also serve as a barrier to disease proliferation. This current review will summarize and highlight the more common pediatric skeletal diseases involving "weak links."

This article is part of the Topical Collection on *Pediatrics*.

✉ John D. MacKenzie
john.mackenzie@ucsf.edu

[1] Department of Radiology and Biomedical Imaging, University of California San Francisco, 1855 4th Street, Rm C1758P, San Francisco, CA 94143, USA

Transition Between Bone and Cartilage

The transition between bone and cartilage is a focal area of weakness susceptible to traumatic disease. A geologic fault line between tectonic plates is an appropriate analogy for why tissue transitions are commonly involved in injury and disease to the pediatric skeleton (Fig. 1a), and several regions of the growing skeleton have unique bone and cartilage transitions (Fig. 1b), which may be susceptible to injury. These regions are affected by acute trauma and chronic repetitive injury, and several well-known examples highlight the injuries at the interface between bone and cartilage (Table 1).

Histology of the Growth Plate

Growth plate consists of chondrocytes arranged in four layers—germinal, proliferative, hypertrophic, and zone of provisional calcification (Fig. 2). The germinal layer is closest to epiphysis, and chondrocytes are in resting stage (not dividing). In the proliferative zone, chondrocytes divide and make columns of cells. In the hypertrophic layer, chondrocytes enlarge and make chondroid (extracellular matrix). In zone of provisional calcification, chondrocytes release calcium to mineralize the matrix and die by apoptosis. Osteoblasts supply osteoid and calcium to ossify the region [1•]. Physeal fractures primarily pass through zone of provisional calcification or hypertrophic zone. However, fracture can extend to germinal zone due to undulating nature of growth plates [1•].

Salter–Harris Fractures

One common injury pattern in the developing skeleton is the growth plate fracture, which accounts for about 15 % of

Table 1 Lesions in children that occur at the interface of different skeletal tissues

Tissue transition	Pathology
Bone and cartilage	
Acute	Salter–Harris
	SCFE
	Patellar sleeve avulsion
	Transitional fractures (triplane, Tillaux)
Chronic	Osteochondritis dissecans
	Physeal injury from repetitive stress
	Little league shoulder
	Little league elbow
	Gymnast wrist and knee
Bone and synchondrosis	Apophyseal avulsion
	Traction apophysitis
	Osgood–Schlatter disease
Tendon/ligament to cartilage/bone	Osgood–Schlatter disease
	Sinding–Larsen–Johansson disease
Transitions in bone	Bowing fractures
Periosteum and bone	Osteomyelitis
	Tumor
	Hemorrhage
	Trauma

all pediatric fractures [2]. These fractures are important to understand because of the risk of growth arrest, which leads to limb length discrepancy or angular deformity. The growth plate (physis) is a continuous transition border between bony metaphysis and cartilaginous epiphysis and is also the weakest part of growing skeleton [1•].

The Salter–Harris system classifies growth plate fracture patterns as types 1, 2, 3, 4, and 5 (Fig. 3). The path of the fracture depicts how energy of the trauma travels through bone and cartilage, and the path tends to travel through the path of least resistance; these are "weak links" in and adjacent to the physis.

The Salter–Harris type 1 fracture involves complete separation of epiphysis from metaphysis without involving surrounding bone [3]. If there is no displacement, radiographic images will most likely be normal as the physis is radiolucent [4]. Type 2 fractures, the most common of the five fracture types, pass through the physis, and angle out through a portion of metaphysis. They are seen in about half of all physeal injuries [5]. The metaphyseal fragment seen in type 2 fragment is a result of failure of fracture to penetrate the tightly attached periosteum to the growth plate [4]. The prognosis of non-displaced type 1 and type 2 Salter–Harris fractures is usually excellent with low risk of growth disturbances [5].

The type 3 fracture runs along the physis and exit through epiphysis. Radiographs are usually sufficient to diagnose type 2 and 3 fractures due to the presence of fracture through the bone of diaphysis and epiphysis, respectively [4]. The type 4 fracture runs from metaphysis to epiphysis across the physis. The type 5 fracture is the rarest of the five fracture types and represents crush injury to the physis [4]. It is typically identified only via MR imaging. The prognoses of type 4 and 5 fractures are comparably worse than those of types 1–3, with more frequent complications [4].

Triplane and Tillaux fractures occur at a unique period of skeletal development and further illustrate the respective weak and strong areas of the pediatric skeleton. The energy

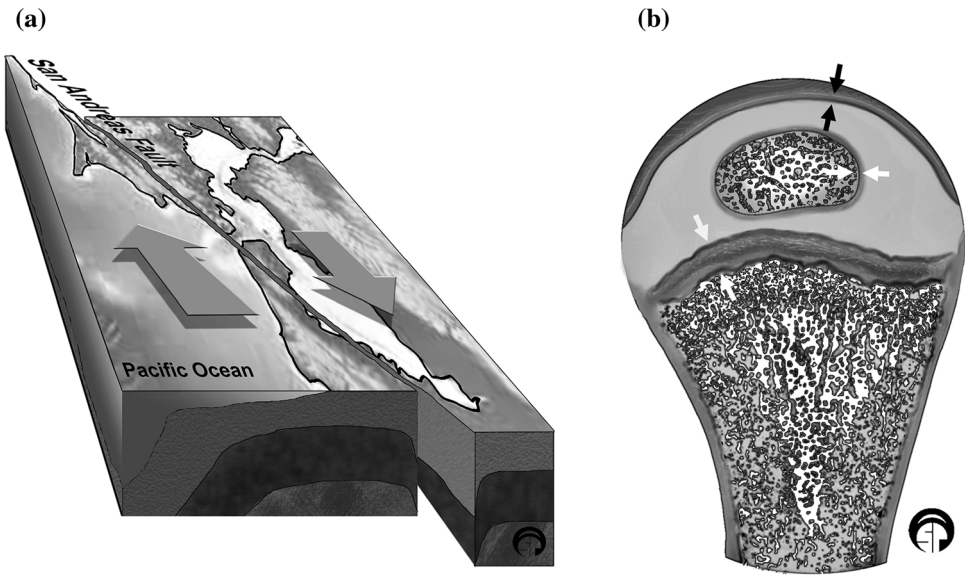

Fig. 1 The geology of the San Andreas Fault (**a**) explained by the interface and movement of two tectonic plates and is responsible for slow changes in topography as well as sudden earthquakes. This fault line is a useful analogy to understand how tissue transitions such as the interface between bone and cartilage serve as a focus for injury (*arrows* in **b**) in the pediatric skeleton

Fig. 2 Histologic section showing the tissue transitions between bone and cartilage at the ossified epiphysis (Epi) → cartilaginous physis (Ph) → ossified metaphysis (Met). Representative specimen from a rodent, which appears identical to a human growth zone

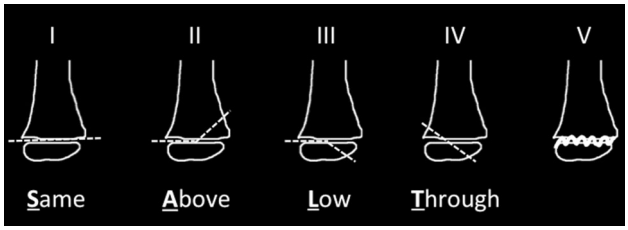

Fig. 3 Schematic of the Salter–Harris fracture classification. *Dashed lines* show the relationship of the fracture with the physis

produced by trauma preferentially travels through areas of skeletal weakness. These transitional fractures occur just prior to complete closure of the physis. The energy of the trauma disrupts open areas of the physis but spares the fused portion. An example is the triplane fracture: as the medial portion of the physis has fused, the medial epiphysis will remain with the metaphysis. However, the lateral aspect of the distal tibial physis is still unfused, and the fracture travels through this region causing displacement of the lateral portion of the epiphysis (Fig. 4).

Formation of a bone bridge (or bone bar) is a common complication after physeal fracture, occurring in ~15 % of all physeal fractures [6]. Transphyseal vascular communication commonly leads to formation of bone bridges [7–9]. Normally, the germinal layer of physis is supplied by epiphyseal vessels, and hypertrophic and ZPC layers are supplied by metaphyseal vessels. Cartilage in physis secretes antiangiogenic factors that prevent communication

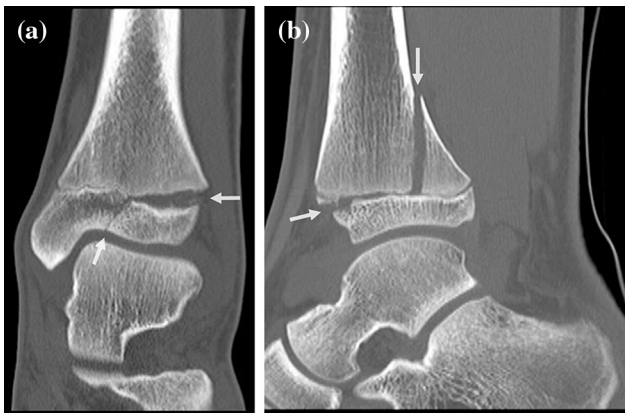

Fig. 4 The triplane fracture, a transitional fracture that illustrates how the energy of the trauma produces fractures in three planes of skeletal weakness. The strong fused physis at the medial aspect of the distal tibia remains intact, whereas the distal fragment displaces due to its relatively weak attachment at the open physis. *Arrows* show the fracture in the axial, coronal, and sagittal planes

of epiphyseal and metaphyseal vessels. Disruption of growth plate may cause transphyseal vascular communication, and subsequent extravasation of osteoprogenitor cells may lead to bone bridge formation [8, 9]. Other mechanisms of bone bridge formation include (1) displacement fractures where epiphyseal bone directly contacts metaphyseal bone and (2) compromise of the vascular supply to the germinal layer [1•].

In vertical fractures perpendicular to the physis, bone bridges form in ~75 % of cases because they allow transphyseal vascularity. However, 25 % of horizontal fractures parallel to the physis develop into bony bridges [7]. Type 4 fractures have the highest prevalence of bridge formation [4]. However, development of a bone bridge is contingent on the degree of physis involvement and the path of fracture than on the Salter–Harris classification [7].

Growth plate arrest due to bridge formation can be complete or partial. Partial bone bridges are classified into three types [10, 11]. In type 1 (peripheral bridge), the bone bridge is in the periphery of the growth plate and can lead to angular as well as limb length deformity. In type 2 (linear bridge), the connection between two-mismatched portions of bone across the growth plate can lead to severe angular deformity. In type 3 (central bridge), the bone bridge is in the center and is surrounded by normal physis. This can result in cupping of the physis and retardation of longitudinal bone growth [1•].

Radiography is the first-line modality to visualize bone bridges. Broken lucency of physis is the main finding; other findings include indistinct physeal margins, epiphyseal displacement, and joint asymmetry. Limitations include inability to identify extent of bar formation, leading to under/overestimation of bar size based on positioning and

projection angle [1•]. CT provides improved detection of physeal bar size, location and extent; however, it is unable to detect early fibrous bone bars [1•].

Due to superior soft tissue contrast, MRI can visualize early fibrous bars difficult to detect on other imaging. Gufer et al. [12] performed MRI on 24 children suffering acute joint trauma without fracture on radiography, but with open physis, limitation of weight-bearing ability, and swelling and tenderness around joint. MRI detected physeal fracture in 34.8 % of these cases. This demonstrates the value of MRI in detecting occult physeal fractures. A fluid-sensitive 3D gradient-recalled echo is a valuable sequence to visualize physeal bars [1•]. Fluid weighting emphasizes cartilage and 3D imaging provides the opportunity to map regions of bone with surrounding residual physeal cartilage and helps plan for potential surgical resection of the bar (Fig. 5).

Slipped Capital Femoral Epiphysis (SCFE)

SCFE is an acute fracture at cartilage bone interface of the hip where capital femoral epiphysis is displaced from the femoral neck at the physis due to mechanical overload [13]. SCFE is a highly common hip disorder in adolescents [14]. The thinning of perichondrial ring around the physis occurring in adolescence may be the reason for its high prevalence in this age group [13]. Recent evidence has shown that body mass, type of physical activity, and the presence of perichondrial ring rather than thickness and inclination of physis are more likely to influence SCFE etiology [15]. SCFE is considered an orthopedic emergency [16, 17], and its most common complication is avascular necrosis of femoral head (prevalence of 5–47 %) [18•].

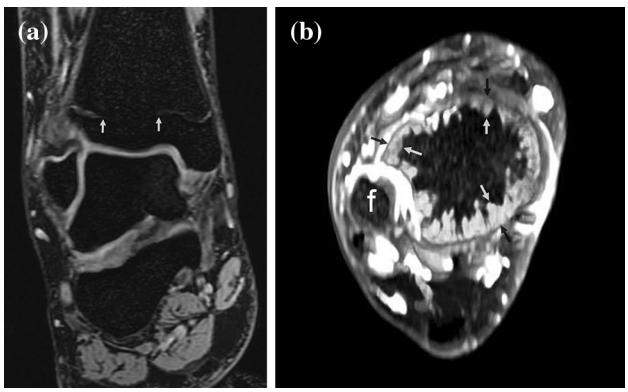

Fig. 5 Three-dimensional high-resolution T2-weighted MRI (**a**) showing the formation of a bone bar. The bright signal intensity of physeal cartilage ends (*arrows*) at the bone bar in the central portion of the tibial physis. The maximum intensity projection image of this 3D dataset (**b**) shows the residual rim of physeal cartilage at the periphery of the tibia (*arrows*) and extent of the bone bar (*black* in center of tibia). The map helps guide decisions. This map shows a large bone bar that was treated conservatively. The map of small lesions helps guide surgery. *f* fibula

Radiography is the primary imaging modality used to diagnose SCFE. Most of the epiphysis slips are posterior with some degree of medial displacement. Valgus slips—displacement of the femoral head superior-laterally and posteriorly—are rare. Posterior slip is assessed with high sensitivity using frog lateral view or true lateral view. Medial slip is assessed using AP view [17, 19].

CT provides little additional value beyond radiography for the diagnosis of SCFE, but 3D models can help in presurgical and planning and postsurgical assessment during serious slips [20]. Ultrasound can assist in the visualization of joint effusion in SCFE but is no better than frog lateral view for assessment of anatomy [21].

MRI is useful either in early cases of SCFE when occult on radiographs and in severe cases where understanding of detailed anatomy is necessary for patient management. MRI findings include physeal widening, bone marrow edema, joint effusion, and synovitis [13, 22]. Based on the severity, slips are classified stable (mild slip) and unstable (severe slip). Devascularization of femoral head occurs only in unstable slips and has high probability of avascular necrosis. Recent evidence has shown perfusion MRI as valuable tool for evaluation of avascular necrosis, especially in an unstable slip [14]. Edouard et al. [14] used dynamic gadolinium-enhanced subtraction techniques on 18 children and reported ability to visualize epiphyseal marrow enhancement with high contrast and space resolution—indicative of vascularization.

Surgical management with screw placement using intraoperative fluoroscopic imaging is performed in most cases of SCFE to stabilize the epiphysis [16]. Emerging computer navigation techniques allow for more accurate screw placement compared to traditional fluoroscopy but do not show evidence of reducing radiation exposure, number of pin passes, or operative time [23].

Osteochondritis Dissecans (OCD)

Is an example of chronic injury at the cartilage–bone interface in the joint. In OCD, a piece of articular cartilage dislodges partially or completely along with the attached subchondral bone. OCD is mainly found in the knee and is bilateral in 15 % of the cases [24]. Other sites include elbow, wrist, hip, and ankle [25]. Pathophysiology of OCD is unclear, but disruption in epiphyseal blood flow due to repeated microtrauma is assumed to play primary role [26, 27].

OCD is diagnosed mainly by imaging as many lesions may be asymptomatic until dislodging occurs. Radiographs are traditionally the first-line imaging and can identify most cases of OCD using four views—anterior–posterior (AP),

lateral, tunnel, and merchant views [25, 28]. However, radiographs underestimate fragment size [29], cannot access status of overlying cartilage [30], and are inferior at distinguishing OCD from an otherwise irregular ossification center [31], which reduces its prognostic and therapeutic value. Prognosis of OCD largely depends on stability of osteochondral fragment and status of overlying articular cartilage [32].

CT provides excellent anatomic view but is poor at analyzing articular cartilage, limiting its value in predicting lesion stability and healing potential. CT arthrography, where iodine contrast is injected in joint and CT scan is taken, provides better view of articular cartilage integrity [25]. Scintigraphy, a nuclear medicine scan procedure, can provide information about blood flow to the lesion [28] but is unsuitable to access integrity of articular cartilage [32].

MRI provides excellent view of intra-articular structures including involvement of the subchondral bone and hyaline cartilage, and thus is ideal for OCD diagnosis and follow-up. MRI-specific findings include cyst-like foci, bone marrow edema, thick epiphyseal cartilage, breaks in subchondral bone, and laminar signal intensity pattern [33••] (Fig. 6a, b). MRI arthrography provides the additional benefits of distention, increased signal/noise ratio, and increased intra-articular pressure [25].

Importantly, MRI is sensitive to subtle differences between OCD and normal variation at the posterior aspect of the femoral condyle [34] (Fig. 6c, d). Further, stable OCD has an intact articular surface whereas unstable OCD is defined as a lesion with fractured or separated cartilage from underlying subchondral bone [28]. Stability is believed to be one of the most important prognostic factors; while stable OCD usually heals with conservative therapy [26, 35], unstable OCD has poorer prognosis [26]. Similarly, juvenile OCD (OCD present during open growth plate) has a much better prognosis compared to adult OCD (growth plate closed). Even though consensus about appropriate treatment is lacking, stable OCD is usually treated non-surgically, while unstable OCD is treated surgically [28, 33••]. Other factors indicating surgery include failure of non-surgical treatment and lesion nearing physeal closure [36].

Criteria for unstable OCD as described by De Smet and colleagues [35] on a T2-weighted MRI include: a high signal intensity rim surrounding the lesion, cysts surrounding the lesion, articular cartilage fracture, and fluid-filled osteochondral defect. T2-weighted MRI had a sensitivity and specificity of 0.97 and 1 respectively in adult patients [35]. Kijowski and colleagues [26] revised De Smet criteria to describe MR finding in juvenile patients when T2-weighted imaging is used: cysts surrounding lesion indicate instability only if they were >5 mm or multiple. Additionally, a high signal line surrounding the OCD lesion indicates instability only if the signal intensity matches the adjacent joint fluid is surrounded by a second low intensity line or occurred together with multiple breaks in subchondral bone plate. The sensitivity and specificity of Kijowski criteria are 100 and 11 %, respectively [26].

Zbojniewicz and colleagues [33••] correlated the histopathology and MRI findings of OCD lesion from a distal femoral biopsy. Biopsy revealed thickened articular cartilage, abundant fibrovascular tissue in the chondroosseous junction insinuating into the trabeculae of bone, and linear cleft space in the cartilage–bone interface. Cyst-like foci on the MRI corresponded to the fibrovascular tissue, and cleft space corresponded to the high signal line between the lesion and normal bone.

Arthroscopy is the gold standard for OCD diagnosis [27]. Its findings are classified into four stages [37] by Dipaola et al.: stage I (soft and irregular cartilage without definable fragment), stage II (breach in articular cartilage with definable but non-displaceable fragment), stage III (displaceable fragment but still attached), and stage IV (loose fragment). Recently, Robach et al. [27] compared MRI findings with arthroscopy findings in 63 cases of juvenile OCD and found that the accuracy of MRI in identifying OCD stage (as classified by Dipaola) was only 41.3 %. This study illustrates the difficulty in predicting

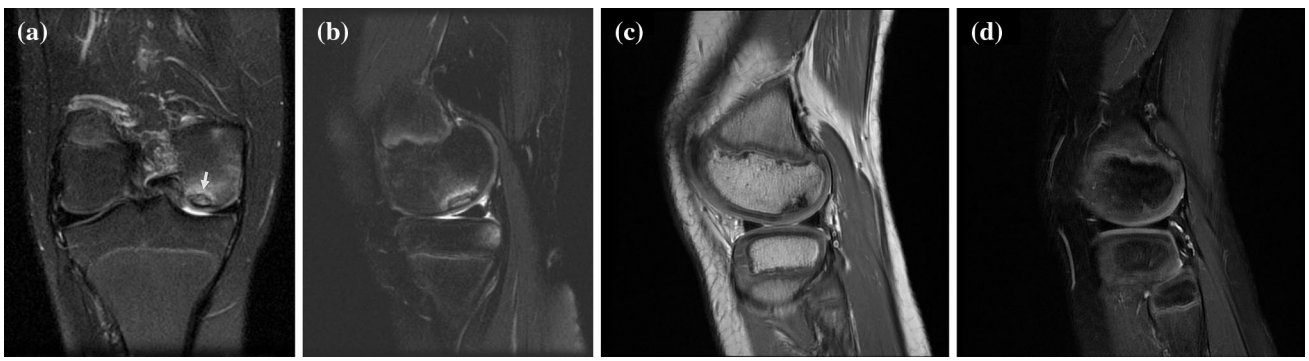

Fig. 6 MRI of osteochondritis dissecans in a 13-year-old girl (**a**, **b**) versus variation of normal developmental anatomy in a separate patient (**c**, **d**)

OCD staging in children and informs the clinician to not make treatment decisions solely based on MRI findings. However, treatment of OCD for juvenile patients is usually performed conservatively as they have good prognosis; surgery is sought only in cases of unstable lesions or conservative treatment failure [27].

Transition Between Bone and Synchondrosis

The apophyseal plate is another area of relative weakness susceptible to injury in the pediatric skeleton. The apophysis is a normal developmental outgrowth of bone and serves as an attachment site for tendons and ligaments. The apophysis joins with the remainder of the bone via the apophyseal plate, which is composed of cartilage and allows for growth of the apophysis. A synchondrosis, which is a fibrotic or cartilaginous bridge between two bones, is another term used to describe the apophyseal plate. The apophyseal plate is two to five times weaker than ligaments and tendons; therefore, a traumatic force is more likely to cause injury to the apophysis and plate rather than the ligament/tendon [38].

Two mechanisms lead to injury of the apophysis—acute epiphyseal avulsion where apophysis separates from bone at the epiphyseal plate, and chronic repetitive trauma which leads to inflammation. The chronic apophysitis (or traction apophysitis) is caused by repetitive tension from tendon or ligament attached to apophysis [39]. Prognosis of apophysitis is excellent following rest and decreasing intensity of activity [40]. Acute avulsion may be the result of underlying weakness from repetitive injury (Fig. 7), usually in children who participate in throwing sports.

Apophysitis is more common in young athletes. It most commonly occurs in calcaneus (Sever's disease) and tibial tubercle from sports including running and sudden change in direction but can also occur in the upper limb from swimming or throwing sports [39]. Other sites for apophysitis include the inferior patellar pole (Sinding–Larsen–Johansson syndrome), iliac crest, anterior superior and anterior inferior iliac spine, ischial tuberosity, greater trochanter, and os naviculare at the attachment of the posterior tibial tendon (Fig. 8).

For imaging of apophysitis, different cases of apophysitis have slightly different characters based on anatomy and location. Radiography and CT show widening of the synchondrosis and adjacent subchondral sclerosis. Ultrasound is usually not helpful since the lesion involves bone. MR demonstrates widening of, and edema in, the

Fig. 8 Painful os navicular axial T2 fat-saturated (**a**) and T1-weighted MRI (**b**) showing bone marrow edema adjacent to the synchondrosis of the os navicular (*arrow*)

Fig. 7 Avulsion of the apophysis of the medial epicondyle in an 11-year-old baseball pitcher. Normal side for comparison (**a**) to the affected side (**b** and **c**) where the epicondyle is separated from the distal humerus on radiography (**b**) and has edema at the site of separation (**c**) on MRI

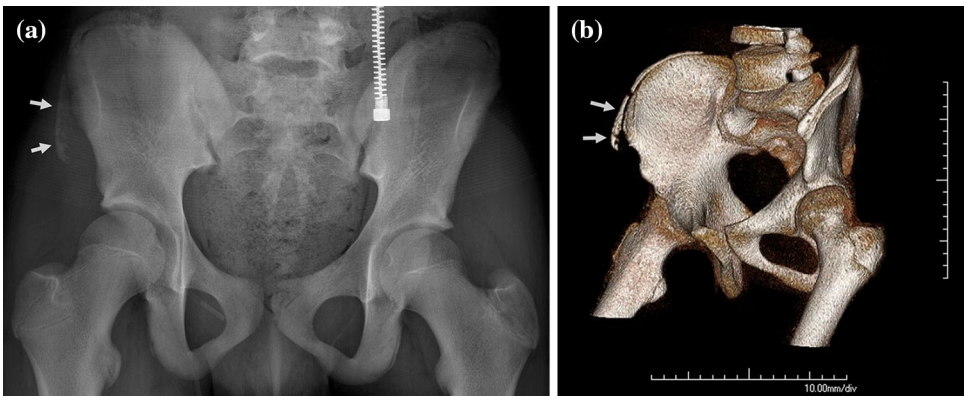

Fig. 9 A 15-year-old boy with anterior superior iliac spine avulsion on radiography (**a**) and 3D CT (**b**). Avulsion injuries in the pediatric pelvis occur at the junction of the apophysis, synchondrosis, and more central bone and are the result of mechanical forces of the tendon at this weak link

synchondrosis; furthermore, bone marrow edema with increased signal intensity on water sensitive sequences in the apophysis and adjacent bone marrow are seen along with fibrous periapophyseal structures. Additionally, contrast enhancement usually follows a similar distribution and pattern as the edema depicted on the fluid-sensitive sequences [39].

Chronic trauma in traction apophysitis disrupts metaphyseal and apophyseal vessels which supplies nutrients to the physis for calcification and transition to bone. The mechanism here may be similar as at the growth plate—where lack of nutrients results in long column of hypertrophic chondrocytes extending from the physis to metaphysis, which in turn causes physeal widening [18•]. This widening can be seen on MRI and commonly resolves after mechanical stressor is taken away. If stressor is not taken away, it can form bone callus that might be mistaken for neoplasm or infection by MRI. This process is common in the pelvis with avulsions at several attachments for tendons (Fig. 9).

Conclusion

The cartilage–bone interface is uniquely at risk for injury in the pediatric skeleton. Transitions from bone to physeal cartilage or around the bone and synchondrosis boundary are affected by acute trauma or chronic repetitive processes that slowly disrupt these weak links. Injuries range from the well-described acute Salter–Harris fractures and apophyseal avulsion injuries to traction apophysitis from chronic repetitive trauma. Transitional fractures also illustrate the areas of relative weakness and future adult strength around the week open physis and strong, partially closed physis. Understanding of this anatomy is critical in the performance and interpretation of pediatric musculoskeletal imaging examinations.

Compliance with Ethical Guidelines

Conflict of Interest Sagar Wagle and Andrew S. Phelps each declare no potential conflicts of interest. John D. MacKenzie reports grants from GE Healthcare.

Human and Animal Rights and Informed Consent This article does not contain any studies with human or animal subjects performed by any of the authors.

References

Papers of particular interest, published recently, have been highlighted as:
- • Of importance
- •• Of major importance

1. • Wang DC, Deeney V, Roach JW, Shah AJ. Imaging of physeal bars in children. Pediatr Radiol. 2015;45:1403–12. *This article reviews normal histology of growth plate of cartilage and describes the pathophysiology of physeal bar formation. In addition, the paper also discusses utility, strength and weaknesses of multiple imaging modalities in evaluating physeal bars. Physeal bars are important clinical complication of fractures passing through growth plates. It can significantly affect bone growth and skeletal maturation. Learning pathophysiology and imaging of physeal bars is important to evaluate patients at risk and guide their treatment.*
2. Mizuta T, Benson WM, Foster BK, Paterson DC, Morris LL. Statistical analysis of the incidence of physeal injuries. J Pediatr Orthop. 1987;7:518–23.
3. Salter RB, Harris WR. Injuries involving the epiphyseal plate. J Bone Joint Surg Am. 1963;45:587–622.
4. Little JT, Klionsky NB, Chaturvedi A, Soral A, Chaturvedi A. Pediatric distal forearm and wrist injury: an imaging review. Radiographics. 2014;34:472–90.
5. Chasm RM, Swencki SA. Pediatric orthopedic emergencies. Emerg Med Clin N Am. 2010;28:907–26.
6. Peterson HA. Physeal and apophyseal injuries. Fractures in children, vol. 3. Philadelphia: Lippincot; 1996. p. 103–65.

7. Ecklund K, Jaramillo D. Imaging of growth disturbance in children. Radiol Clin N Am. 2001;39:823–41.
8. Xian CJ, Zhou FH, McCarty RC, Foster BK. Intramembranous ossification mechanism for bone bridge formation at the growth plate cartilage injury site. J Orthop Res. 2004;22:417–26.
9. Jaramillo D, Shapiro F, Hoffer FA, Winalski CS, Koskinen MF, Frasso R, et al. Posttraumatic growth-plate abnormalities: MR imaging of bony-bridge formation in rabbits. Radiology. 1990;175:767–73.
10. Ogden JA. The evaluation and treatment of partial physeal arrest. J Bone Joint Surg Am. 1987;69:1297–302.
11. Escott BG, Kelley SP. Management of traumatic physeal growth arrest. Orthop Trauma. 2012;26:200–11.
12. Gufler H, Schulze CG, Wagner S, Baumbach L. MRI for occult physeal fracture detection in children and adolescents. Acta Radiol. 2013;54:467–72.
13. Georgiadis AG, Zaltz I. Slipped capital femoral epiphysis: how to evaluate with a review and update of treatment. Pediatr Clin N Am. 2014;61:1119–35.
14. Edouard C, Raphaël V, Hubert DLP. Is the femoral head dead or alive before surgery of slipped capital femoral epiphysis? Interest of perfusion magnetic resonance imaging. J Clin Orthop Trauma. 2014;5:18–26.
15. Castro-Abril HA, Galván F, Garzón-Alvarado DA. Geometrical and mechanical factors that influence slipped capital femoral epiphysis: a finite element study. J Pediatr Orthop B. 2015;24:418–24.
16. Koutenaei BA, Guler O, Wilson E, Thoranaghatte RU, Oetgen M, Navab N, et al. Improved screw placement for slipped capital femoral epiphysis (SCFE) using robotically-assisted drill guidance. Med Image Comput Comput Assist Interv. 2014;17:488–95.
17. Jarrett DY, Matheney T, Kleinman PK. Imaging SCFE: diagnosis, treatment and complications. Pediatr Radiol. 2013;43(Suppl 1):S71–82.
18. • Chang GH, Paz DA, Dwek JR, Chung CB. Lower extremity overuse injuries in pediatric athletes: clinical presentation, imaging findings, and treatment. Clin Imaging. 2013;37:836–46. *This article talks about overuse injury of lower extremity in pediatric athletes. Pathogenesis of these injuries are discussed. In addition, the utility of multiple imaging modalities including radiograph, CT, MRI for multiple acute and chronic overuse injury are discussed. Knowledge of pathogenesis and importance of imaging techniques can help in patient management.*
19. Billing L, Bogren HG, Wallin J. Reliable X-ray diagnosis of slipped capital femoral epiphysis by combining the conventional and a new simplified geometrical method. Pediatr Radiol. 2002;32:423–30.
20. Tins B, Cassar-Pullicino V, McCall I. The role of pre-treatment MRI in established cases of slipped capital femoral epiphysis. Eur J Radiol. 2009;70:570–8.
21. Castriota-Scanderbeg A, Orsi E. Slipped capital femoral epiphysis: ultrasonographic findings. Skelet Radiol. 1993;22:191–3.
22. Umans H, Liebling MS, Moy L, Haramati N, Macy NJ, Pritzker HA. Slipped capital femoral epiphysis: a physeal lesion diagnosed by MRI, with radiographic and CT correlation. Skelet Radiol. 1998;27:139–44.
23. Bono KT, Rubin MD, Jones KC, Riley PM, Ritzman TF, Schrader WC, et al. A prospective comparison of computer-navigated and fluoroscopic-guided in situ fixation of slipped capital femoral epiphysis. J Pediatr Orthop. 2013;33:128–34.
24. Hefti F, Beguiristain J, Krauspe R, Möller-Madsen B, Riccio V, Tschauner C, et al. Osteochondritis dissecans: a multicenter study of the European Pediatric Orthopedic Society. J Pediatr Orthop B. 1999;8:231–45.
25. Moktassi A, Popkin CA, White LM, Murnaghan ML. Imaging of osteochondritis dissecans. Orthop Clin N Am. 2012;43:201–11.
26. Kijowski R. Juvenile versus adult osteochondritis dissecans of the knee: appropriate MR imaging criteria for instability 1. Radiology. 2008;248:571–8.
27. Roßbach BP, Paulus AC, Niethammer TR, Wegener V, Gülecyüz MF, Jansson V, et al. Discrepancy between morphological findings in juvenile osteochondritis dissecans (OCD): a comparison of magnetic resonance imaging (MRI) and arthroscopy. Knee Surg Sports Traumatol Arthrosc. 2015. http://dx.doi.org/10.1007/s00167-015-3724-3.
28. Edmonds EW, Polousky J. A review of knowledge in osteochondritis dissecans: 123 years of minimal evolution from König to the ROCK study group. Clin Orthop Relat Res. 2013;471:1118–26.
29. Bradley J, Dandy DJ. Osteochondritis dissecans and other lesions of the femoral condyles. J Bone Joint Surg Br. 1989;71:518–22.
30. Scott DJ Jr., Stevenson CA. Osteochondritis dissecans of the knee in adults. Clin Orthop Relat Res. 1971;76:82–6.
31. Gebarski K, Hernandez RJ. Stage-I osteochondritis dissecans versus normal variants of ossification in the knee in children. Pediatr Radiol. 2005;35:880–6.
32. Kramer J, Stiglbauer R, Engel A, Prayer L, Imhof H. MR contrast arthrography (MRA) in osteochondrosis dissecans. J Comput Assist Tomogr. 1992;16:254–60.
33. •• Zbojniewicz AM, Stringer KF, Laor T, Wall EJ. Juvenile osteochondritis dissecans: correlation between histopathology and MRI. AJR Am J Roentgenol. 2015;205:W114–23. *In this study, Zbojniewicz and colleagues compared MRI of osteochondritis dissecans (OCD) lesions in five children with their transarticular biopsy. They were able to precisely correlate histopathological overlay with MRI appearance of the lesion. Hence, the researchers advanced the understanding of osteochondritis dissecans which could impact clinical management of patients with OCD.*
34. Laor T, Jaramillo D. MR imaging insights into skeletal maturation: what is normal? Radiology. 2009;250:28–38.
35. De Smet AA, Ilahi OA, Graf BK. Reassessment of the MR criteria for stability of osteochondritis dissecans in the knee and ankle. Skelet Radiol. 1996;25:159–63.
36. Trinh TQ, Harris JD, Flanigan DC. Surgical management of juvenile osteochondritis dissecans of the knee. Knee Surg Sports Traumatol Arthrosc. 2012;20:2419–29.
37. Dipaola JD, Nelson DW, Colville MR. Characterizing osteochondral lesions by magnetic resonance imaging. Arthroscopy. 1991;7:101–4.
38. Young SW, Safran MR. Greater trochanter apophysitis in the adolescent athlete. Clin J Sport Med. 2015;25:e57–8.
39. Arnaiz J, Piedra T, de Lucas EM, Arnaiz AM, Pelaz M, Gomez-Dermit V, et al. Imaging findings of lower limb apophysitis. AJR Am J Roentgenol. 2011;196:W316–25.
40. Bedoya MA, Jaramillo D, Chauvin NA. Overuse injuries in children. Top Magn Reson Imaging. 2015;24:67–81.